Supporting Information

Ordered Mesoporous Graphitized Pyrolytic Carbon Materials: A Comprehensive Study of Synthesis, Graphitization, and Electrochemical Properties

Zhangxiong Wu, [a, b] Wei Li, [b] Yongyao Xia, [b] Paul A Webley, [a] and Dongyuan Zhao* [a, b]

[a] Department of Chemical Engineering, Faculty of Engineering, Monash University, Melbourne, VIC 3800, Australia; [b] Department of Chemistry and Laboratory of Advanced materials, Fudan University, Shanghai 200433, P. R. China.

Email: dyzhao@fudan.edu.cn, Tel: 86-21-5163-0205, Fax: 86-21-5163-0307

1. Details for calculating the Koutecky - Levich plots:

The Koutecky - Levich plots and the kinetic parameters of ORR can be analyzed on the basis of the Koutecky - Levich equations:

$$1/j = 1/j_L + 1/j_K = 1/(B\omega^{1/2}) + 1/j_K \qquad (1)$$

$$B = 0.62nFC_0(D_0)^{3/2}v^{-1/6} \qquad (2)$$

$$j_K = nFkC_0 \qquad (3)$$

where j (mA/cm^2) is the measured current density, j_K and j_L (mA/cm^2) are the kinetic- and diffusion-limiting current densities, ω is the angular velocity of the rotating disk ($\omega = 2\pi N$, N is the linear rotating speed in rpm), n is the overall number of electrons transferred in ORR, F is the Faraday constant, C_0 is the bulk concentration of O_2, D_0 is diffusion coefficient of O_2, v is the kinematic viscosity of the electrolyte, and k is the electron transfer rate constant, respectively. According to the Equations (1) and (2), the number of electrons transferred (n) and the kinetic-limiting current j_K can be obtained from the slope and intercept of the Koutecky–Levich plots ($1/j$ versus $\omega^{-1/2}$).

2. Supporting Figures

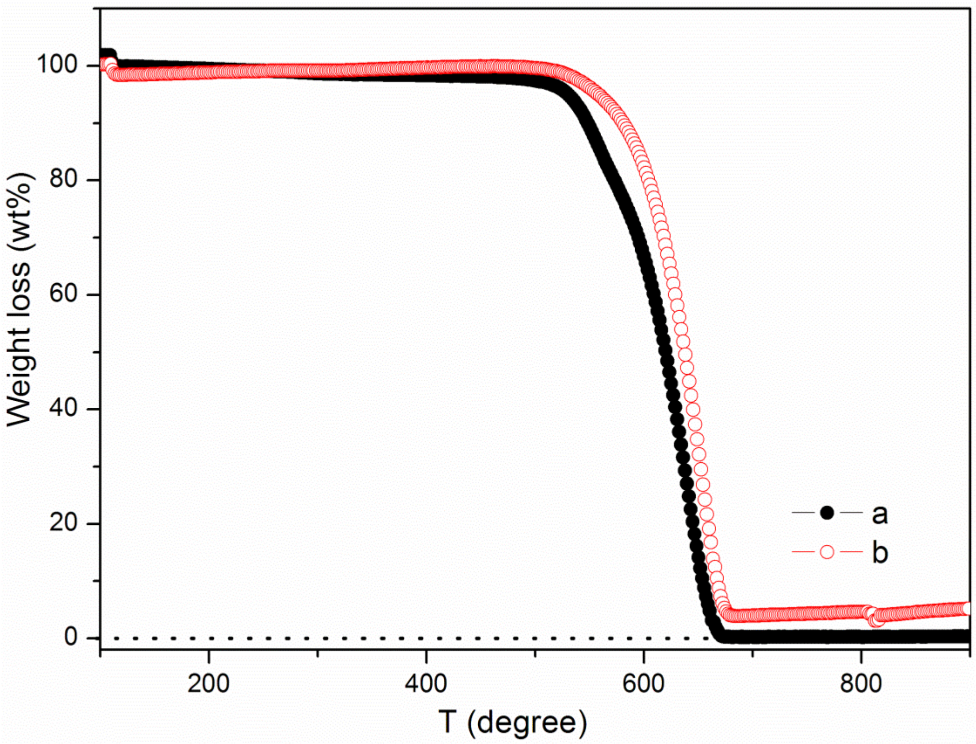

Figure S1. TG curves under flowing O_2 of the mesoporous MGC-SBA-15-900-3h (a) and the resultant mesoporous carbon (b) obtained by heating the GC@SBA-15-900-3h composite at 1000 °C under Ar for 3 h followed by the silica template removal.

It is found that the mesoporous MGC-SBA-15-900-3h can be fully combusted with almost no residue (a), indicating that the silica component is fully removed. However, for the graphitic carbon sample obtained by heating the GC@SBA-15-900-3h composite at 1000 °C under Ar for 3 h followed by the silica template removal, the TG curve (b) shows a small gentle weight increase at room temperature to ~ 500 °C, and meanwhile there is about 3.8 wt% of residue, due to the formation of some silicon carbide compositions during the thermal treatment accounting for the weight increase and the oxidation of silicon carbide with SiO_2 as the residue after combustion. This is why we didn't adopt a higher temperature than 1000 °C to heating the GC@SBA-15 composites for graphitization promotion.

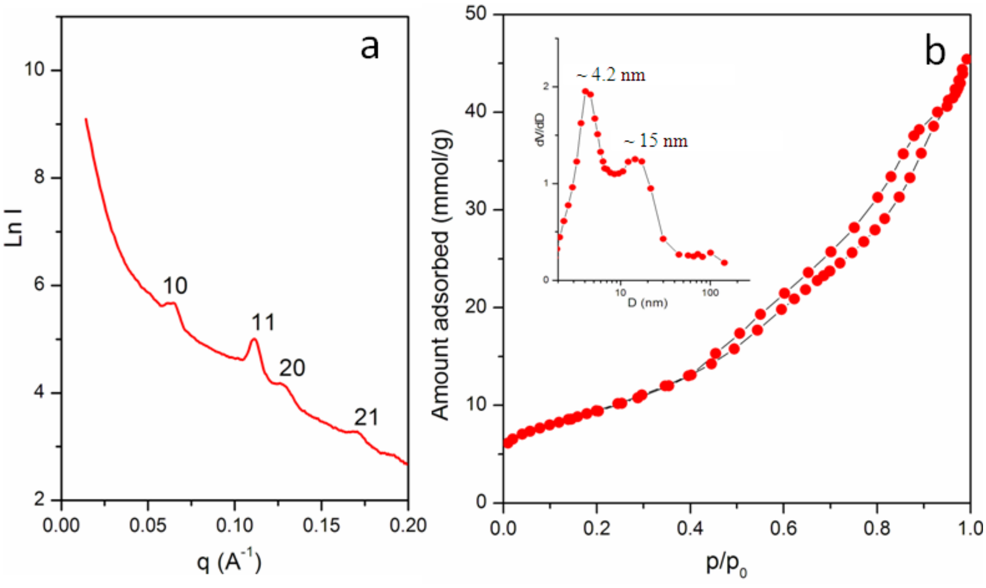

Figure S2. SAXS pattern (a), N_2 sorption isotherms and the inset corresponding pore size distribution (b) of the resultant mesoporous graphitic carbon obtained by the thermal treatment of the mesoporous GC@SBA-15-900-3h composite at 1000 °C for 3 h under Ar atmosphere followed by silica removal.

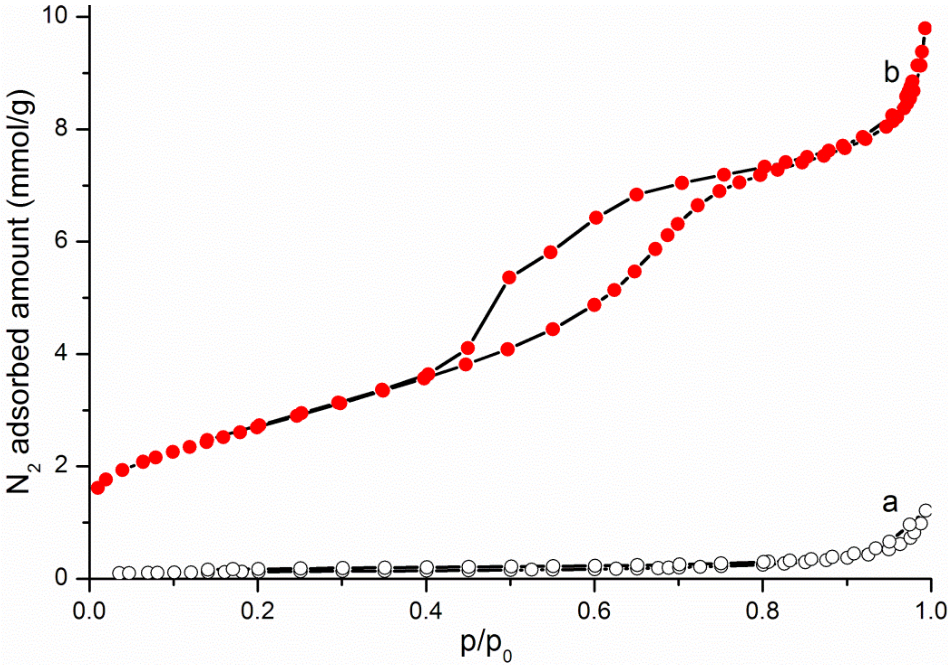

Figure S3. N_2 sorption isotherms of the mesoporous GC@SBA-15-900-3h composite (a) and the resultant composite (b) obtained by heating it at 1000 °C for 3 h under Ar atmosphere.

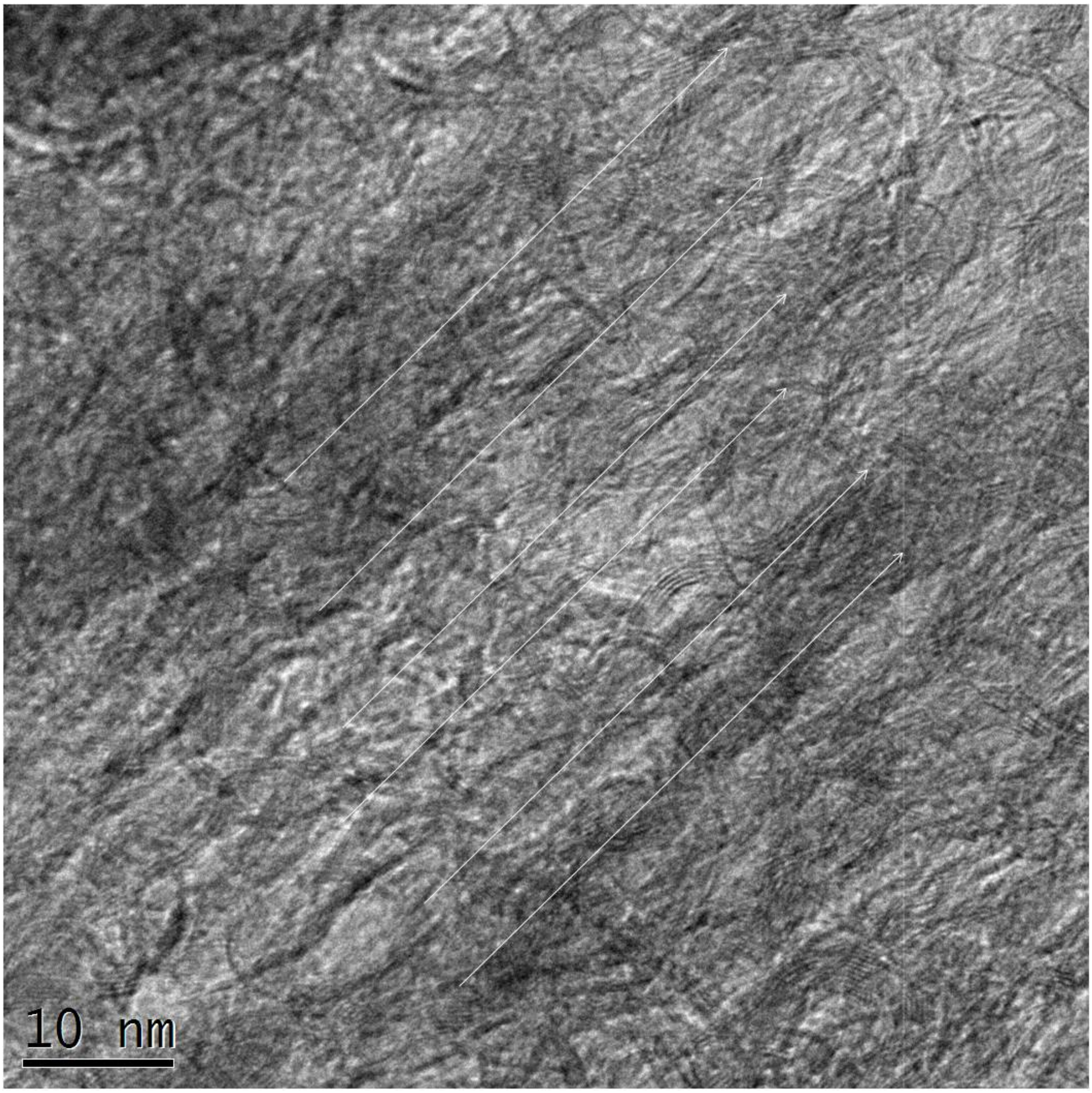

Figure S4. The HRTEM image of the resultant mesoporous graphitic carbon sample obtained by heating the GC@SBA-15-900-3h composite at 1000 °C for 3 h under Ar atmosphere followed by the silica template removal, showing clear (002) plane lattices generally parallel to the long axis of the carbon nanowires.

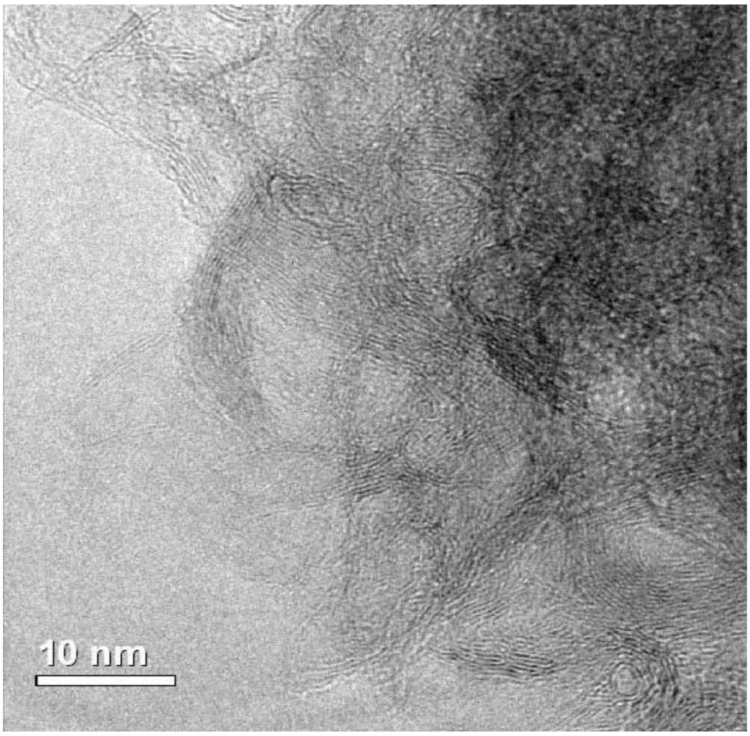

Figure S5. The HRTEM image of the carbon nanoflakes located on the external surface of the carbon mesopore walls of the resultant mesoporous graphitic carbon sample obtained by heating the GC@SBA-15-900-3h composite at 1000 °C for 3 h under Ar atmosphere followed by the silica hard template removal.

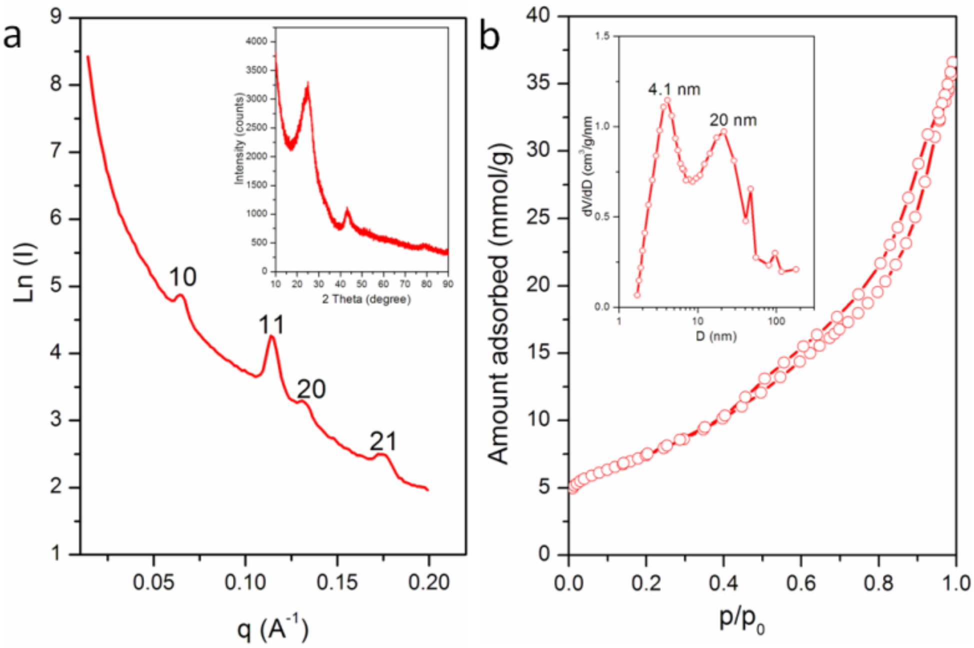

Figure S6. The SAXS (a), Wide-angle XRD (inset in a) patterns and N_2 sorption isotherms (b) and the corresponding pore size distribution (inset in b) of the resultant mesoporous mesoporous graphitic carbon obtained by the graphitization promoting step at 1200 °C for 2 h under vacuum.

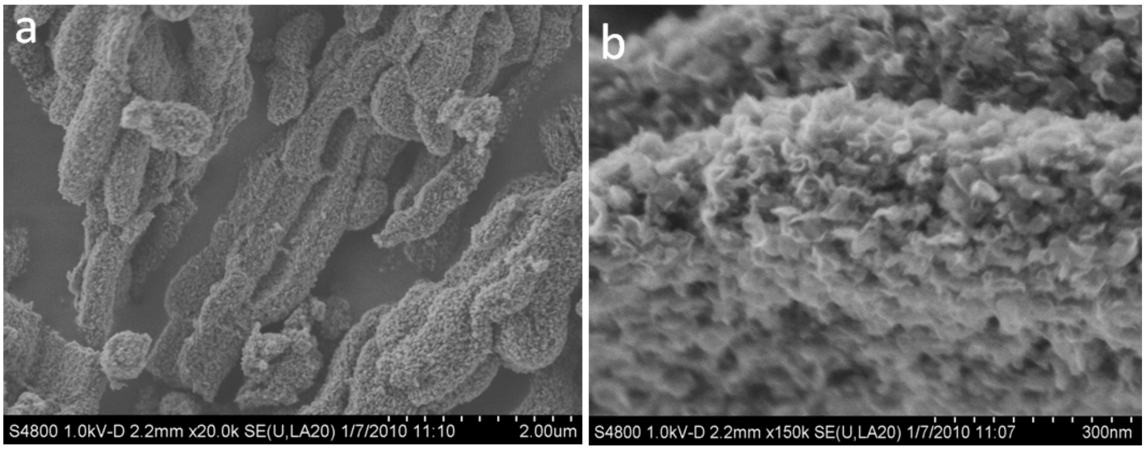

Figure S7. SEM images of the resultant mesoporous graphitic carbon material obtained by the graphitization promoting step at 1200 °C for 2 h under vacuum.

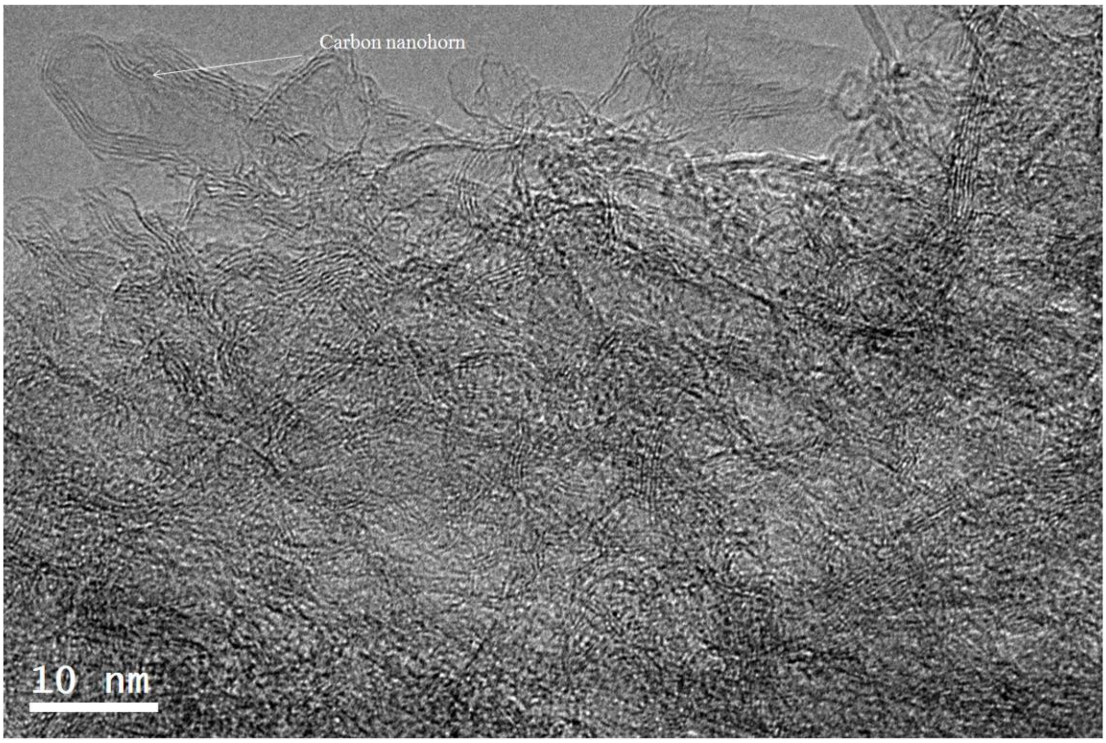

Figure S8. The HRTEM image of the outer layers of the mesopore carbon pore-walls and the carbon nanoflakes or nanohorns of the resultant mesoporous graphitic carbon sample obtained through the graphitization promoting step at ~ 1200 °C under vacuum.

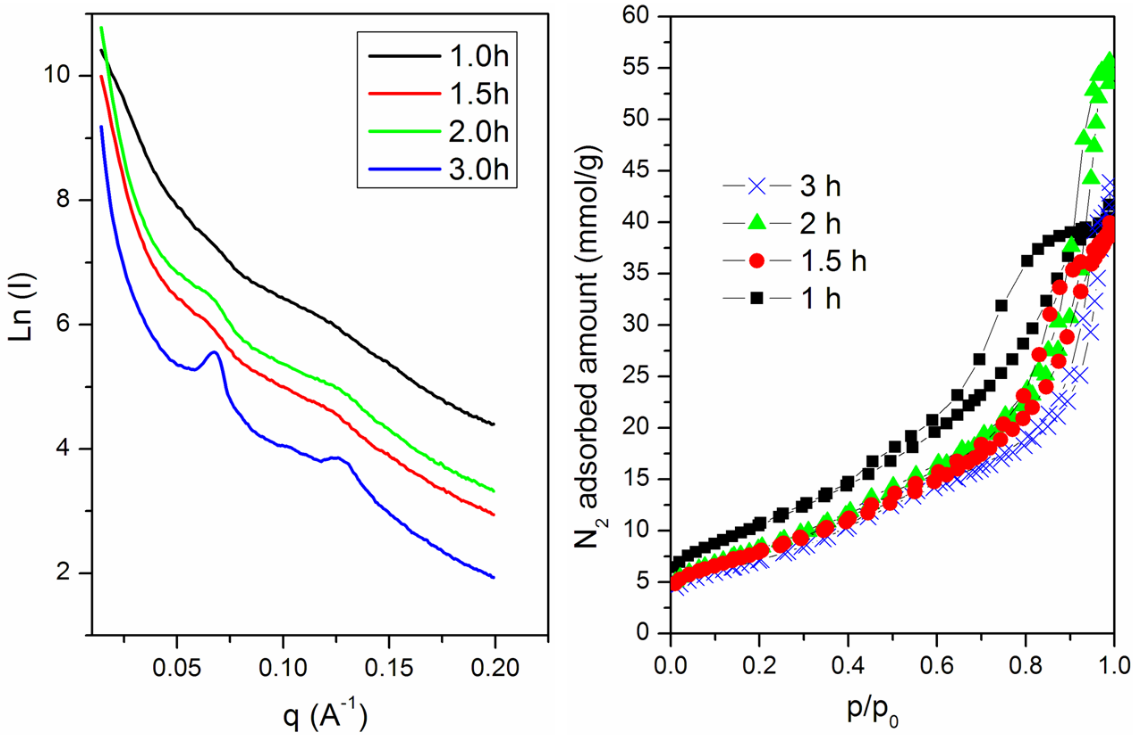

Figure S9. The SAXS patterns (left) and N_2 sorption isotherms (right) of the mesoporous graphitic carbons obtained at 900 °C with a CVD time of 1.0 ~ 3.0 h with the bicontinuous cubic mesoporous silica KIT-6 as a hard template.

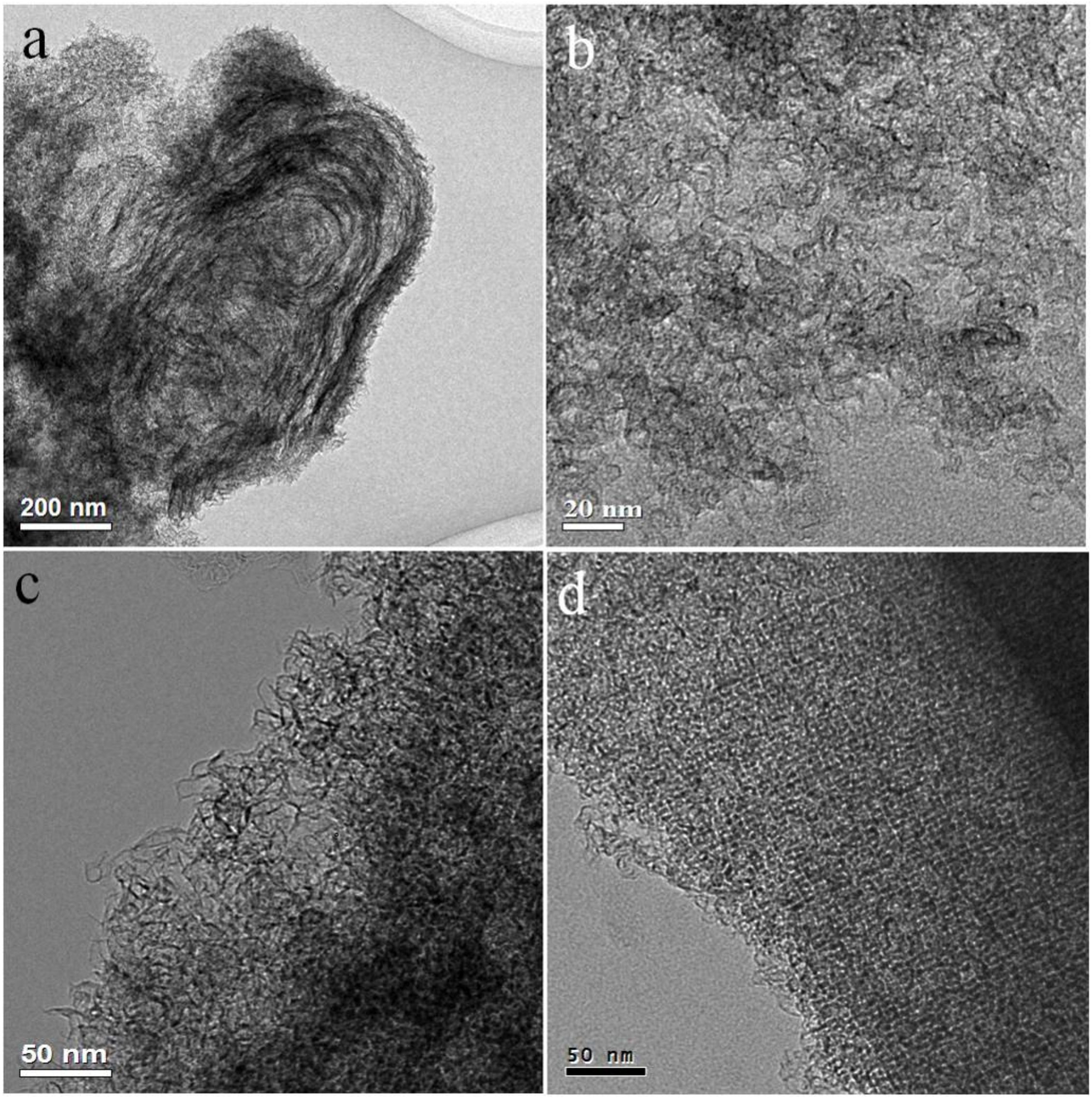

Figure S10. Representative TEM images of the mesoporous graphitic carbons obtained at 900 °C with a CVD time of 1.0 (a), 1.5 (b), 2.0 (c) and 3.0 h (d) with the bicontinuous cubic mesoporous silica KIT-6 as a hard template.

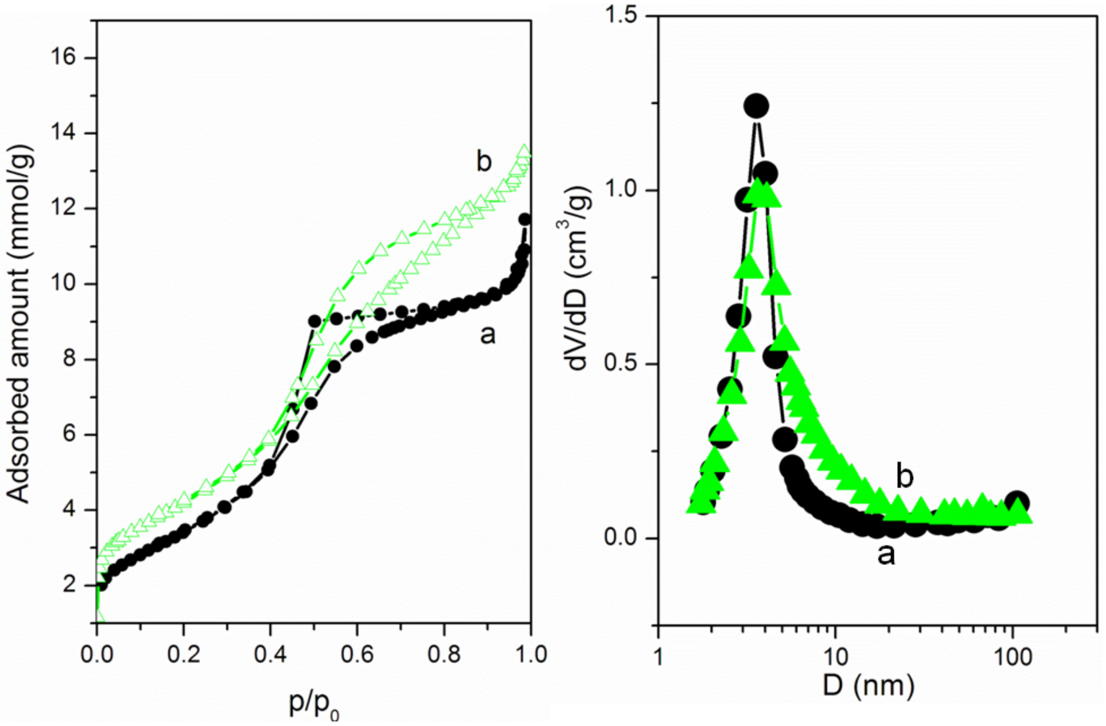

Figure S11. N_2 sorption isotherms (left) and the corresponding pore size distribution curves (right) of the mesoporous composite MGC-SBA-15-900-3h (a) and the resultant carbon supported Pt catalyst (b) with a Pt content of ~ 4.7 wt% (determined by TG analysis).

The isotherms show that after the Pt loading, both the microporosity and mesoporosity are increased, attributed to the decomposition and/or carbothermal reduction of the Pt precursor releasing gaseous products and generating microporosity. The rearrangement and graphitization of the carbon networks can also generate larger mesopore voids.

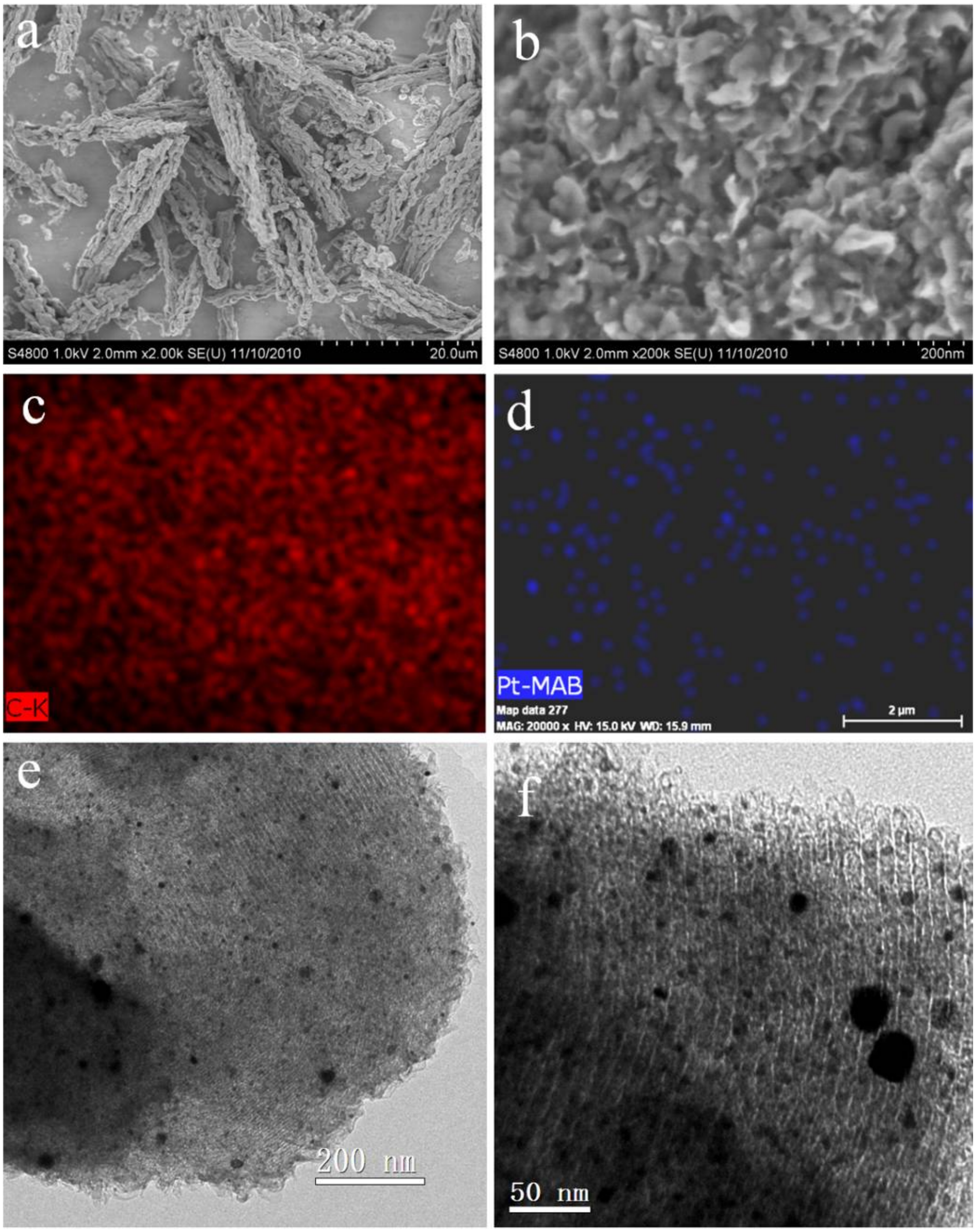

Figure S12. SEM images (a, b), C and Pt elemental mapping results (c, d) and TEM images (e, f) of the mesoporous MGC-SBA-15-900-3h supported Pt catalyst with a Pt content of ~ 4.7 wt%.

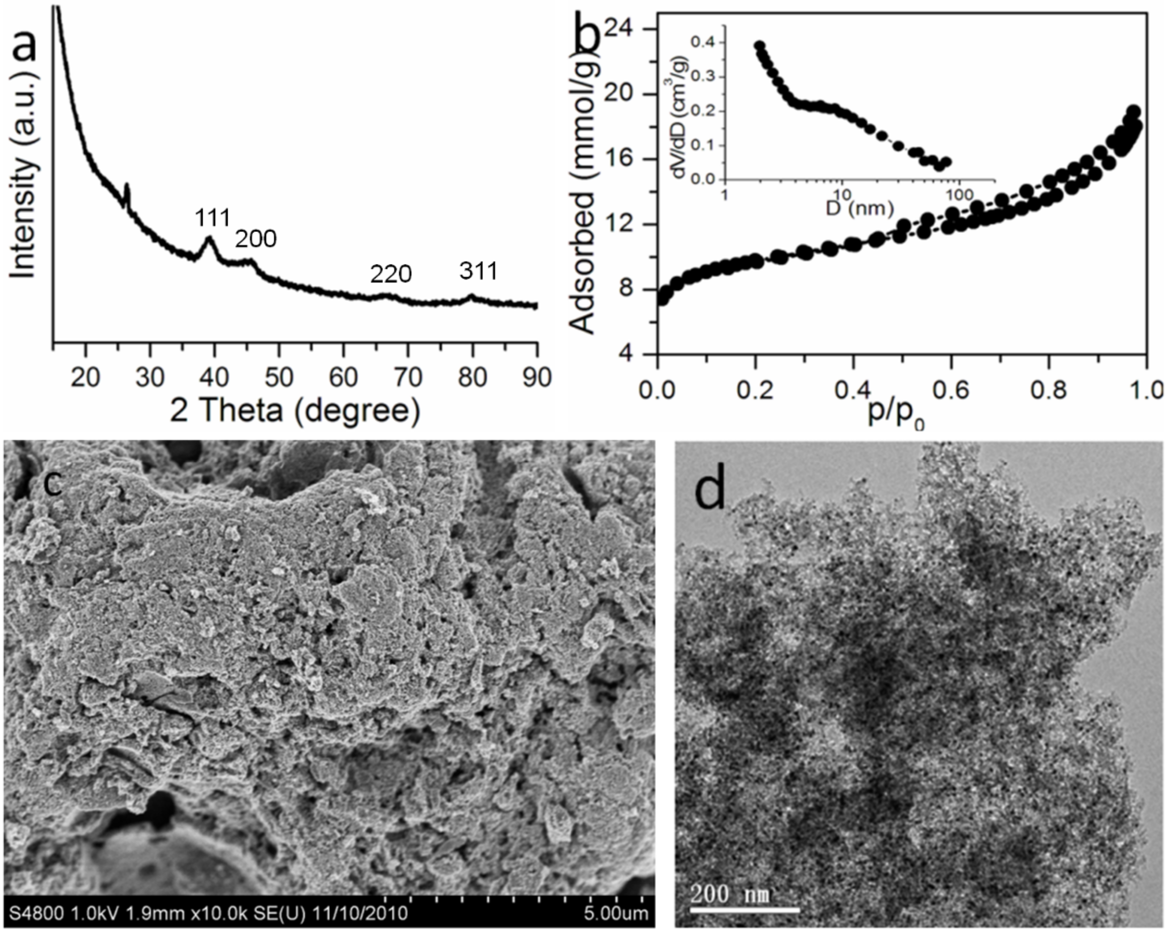

Figure 13. The wide-angle XRD pattern (a), N_2 sorption isotherms (b) together with the pore size distribution curve (inset in b), SEM (c) and TEM (d) images of the comercial activated carbon supported Pt catalyst with a Pt content of ~ 5.6 wt%.

It is found that the sizes of the Pt nanoparticles are mostly ~ 3.5 nm. The N_2 sorption isotherms show that the samples are both microporous and mesoporous. The surface area and pore volume are calculated to be ~ 740 m^2/g and 0.68 cm^3/g, respectively. The SEM and TEM images reveal that the carbon matrix is mainly microporous while the mesopores mainly come from the pore voids between the carbon particles. The TEM image shows direct evidence that the Pt nanoparticles are highly and uniformly dispersed in the carbon support.

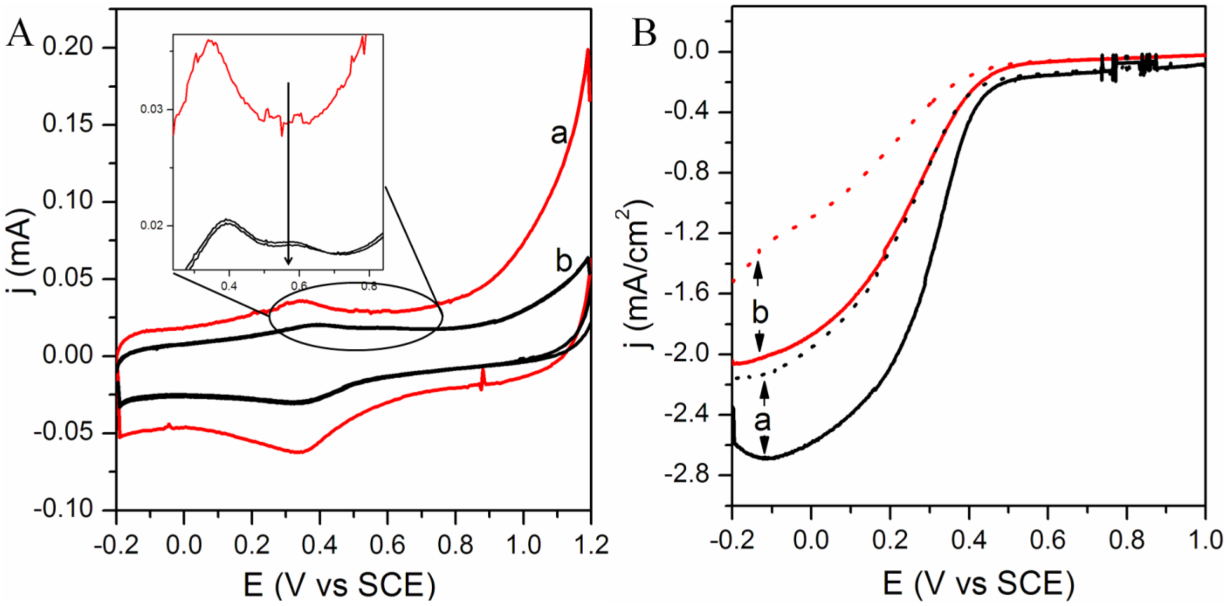

Figure S14. CV curves (A) recorded under N_2-saturated H_2SO_4 electrolyte (0.5 M) in the present of 0.5 M CH_3OH and the polarization curves (1600 rpm) in specific activity (B) recorded under O_2-purging condition of the mesoporous MGC-SBA-15-900-3h supported Pt catalyst with a Pt content of ~ 4.7 wt% (a) and the commercial activated carbon supported catalyst with a Pt content of ~ 5.6 wt% (b). The inset in (A) is the magnified curves showing the methanol oxidation signal marked by an arrow. The solid and dash lines in (B) correspond to the results obtained before and after potential cycling (100 CV cycles). The Pt load of the catalysts on the electrode is ~ 13.5 μg/cm^2.